

Electron-impact study of the S₂ molecule using the *R*-matrix method

Jasmeet Singh Rajvanshi* and K L Baluja†

Department of Physics and Astrophysics, University of Delhi, Delhi 110 007, India

(Received 8 July 2011; published 17 October 2011)

The present study deals with the calculation of elastic [integrated and differential cross section (DCS)], momentum-transfer, excitation, and ionization cross sections for electron impact on S₂ molecules using the *R*-matrix method. The target states are represented by including correlations via a configuration-interaction technique. We used a double zeta plus polarization Gaussian basis set contracted as (12,8,1)/(6,4,1) for S atoms. The results of the static exchange, correlated one-state, and 20-state close-coupling approximations are presented. We have detected a stable anionic bound state ²Π_g of S₂⁻ having the configuration 1σ_g²...5σ_g² 1σ_u²...4σ_u² 1π_u⁴ 1π_g⁴ 2π_u⁴ 2π_g³. The vertical electron affinity value is 1.42 eV, which is comparable with the experimental value of 1.67 ± 0.015 eV. We detected two shape resonances, both of ²Π_u symmetry in the excitation cross sections of the ¹Δ_g and ¹Σ_g⁺ excited states. The dissociative nature of these resonances is explored by performing scattering calculations in which the S-S bond is stretched. These resonances support dissociative attachment, yielding S and S⁻. We have also predicted six resonances of various symmetries (²A_u, ²B_{1g}, ⁴A_u, ⁴B_{1g}) in the X³Σ_g⁻ → B³Σ_u⁻ transition. We have calculated the DCS, in a correlated one-state model, by using the POLYDCS program of Sanna and Gianturco. The data from the momentum-transfer cross section, generated from DCS, are used to compute effective collision frequencies over a wide electron temperature range (200–30 000 K). The ionization cross sections are calculated in the binary-encounter Bethe model in which Hartree-Fock molecular orbitals at a self-consistent level are used to calculate kinetic and binding energies of the occupied molecular orbitals. We have included up to *g*-partial wave (*l* = 4) in the scattering calculations. For this molecule we have used a Born-closure top-up procedure to account for the higher partial waves for the convergence of the cross section for the dipole-allowed excitation from the ground state. We have also evaluated the scattering length of the S₂ molecule, which is equal to 2.615a₀.

DOI: [10.1103/PhysRevA.84.042711](https://doi.org/10.1103/PhysRevA.84.042711)

PACS number(s): 34.80.Bm, 34.80.Gs, 34.80.Ht

I. INTRODUCTION

The study of the electronic structure of sulfur is very important for investigating its properties and applications. The valence shell orbitals of sulfur are 3*s* and 3*p* atomic orbitals. The S₂ molecule has its own astrophysical importance. It has been observed in the atmosphere of Jupiter [1], in comets [2], and in dense molecular clouds [3]. The molecule S₂ is responsible for the bulk of light emitted by the sulfur lamp [4]. The B³Σ_u⁻–X³Σ_g⁻ transition for the S₂ molecule is very intense and is widely observed in flames, shock tubes, and discharges [5].

The valence configuration interaction (VCI) and self-consistent field (SCF) results of O₂ and S₂ were obtained by Tait *et al.* [6] using an identical minimal basis set composed of Slater-type orbitals. The results of SCF and configuration-interaction (CI)-type calculations on 13 low-lying electronic states of diatomic sulfur were reported by Swope *et al.* [7] using a basis set of double-zeta quality augmented with polarization functions. The impact-parameter method for diatomic molecules was used, for optically allowed transitions from the ground electronic state X³Σ_g⁻ to two lower states of ³Σ_u⁻ symmetry and ³Π_u symmetry by Garrett *et al.* [8]. The *ab initio* effective valence shell Hamiltonian of S₂ was calculated as a function of internuclear distance using quasidegenerate

many-body perturbation theory with the full valence space spanned by six valence orbitals 4σ_g, 4σ_u, 5σ_g, 2π_u, 2π_g, 5σ_u [9]. They reported potential curves and excitation energies for several valence states and the results were compared with CI calculations using the same primitive basis. The potential energy curves for 13 lowest electronic states of S₂ were computed [10] at the multireference CI level using complete active space self-consistent field (CASSCF) orbitals with correlation-consistent cc-pVQZ basis set. Recently the electron-impact excitation of S₂ molecules was studied using the fixed-nuclei *R*-matrix method based on state-averaged CASSCF orbitals by Tashiro [11] with the cc-pVTZ basis set. The author [11] included 13 target states, X³Σ_g⁻, a¹Δ_g, b¹Σ_g⁺, c¹Σ_u⁻, A³Δ_u, A³Σ_u⁺, B³Π_g, B³Σ_u⁻, 1¹Π_g, 1¹Δ_u, B³Π_u, 1¹Σ_u⁺, and 1¹Π_u, in the *R*-matrix calculation. The author also reported the integral cross sections, for elastic collision as well as excitation of the seven lowest excited electronic states, and differential cross sections for elastic collision and excitation of a¹Δ_g, b¹Σ_g⁺, and B³Σ_u⁻ states. More recently the total ionization cross sections for S₂ and other molecules (formed by C, O, and S), for energies from threshold to 5000 eV, were reported [12] using the complex spherical potential-ionization contribution method. The ionization cross sections for S₂ and other molecules of sulfur were measured experimentally and reported by Freund *et al.* [13] with an accuracy of ±10%. The total ionization cross sections of 11 molecules, including the S₂ molecule, were presented for incident electron energies from threshold to 1 keV by Kim *et al.* [14] using the binary-encounter-Bethe model with a Gaussian basis set (6-311-G set) provided by

*Also at Physics and Electronics Department, Keshav Mahavidyalaya, University of Delhi, India; rajvanshi_jasmeet@yahoo.co.in

†kl.baluja@yahoo.com

the GAMESS code. An experiment was performed on the dissociative electron attachment of S_2 molecules by Le Coat *et al.* [15].

The present study uses the *ab initio* R -matrix method for low-energy scattering of the S_2 molecule in the fixed-nuclei approximation. The calculations use the UK molecular R -matrix code [16,17]. The R -matrix method has the advantage over other scattering methods in providing cross sections at a large number of scattering energies efficiently. It also has the ability to include correlation effects and gives an adequate representation of several excited states of the molecule [18]. We are interested in the low-energy region (≤ 10 eV), which is a favorite ground for the R -matrix method. The incoming electron can occupy one of the many unoccupied molecular orbitals or can excite any of the occupied molecular orbital as it falls into another one. These processes give rise to the phenomenon of resonances forming a negative molecular ion for a finite time before the resonance decays into energetically open channels.

Electron-scattering calculations are performed at static exchange, one-state CI, and close-coupling approximations in which we have retained 20 target states in the R -matrix formalism. The integrated elastic and the differential and momentum cross sections for electron impact on an S_2 molecule from its ground state are reported. The excitation cross sections from the ground state to a few low-lying excited states have also been calculated. We have also computed the binary-encounter-Bethe (BEB) ionization cross section [19,20]. The BEB cross sections depend only on the binding energies, the kinetic energies, and the occupation number of the occupied molecular orbitals of the target, and on the energy of the incident electron. The momentum-transfer cross sections calculated in the R -matrix approximation have been used to calculate the effective collision frequency over a wide electron temperature range. We have also evaluated the scattering length of the S_2 molecule. In this procedure we have included only s waves which means only s orbitals are contributing. We must point out that the R -matrix approach is not the only scattering method that allows the *ab initio* inclusion of correlation effects and for studies of open-shell targets. The complex Kohn variational method has been successfully employed for polyatomic targets [21].

II. METHOD

A. Theory

Since the R -matrix theory has been described in detail elsewhere [22,23], we only give an outline here. In an R -matrix approach, there are two distinct physically separated spatial regions, an inner region and an outer region, that are defined with respect to electron-molecule distances. These are treated differently in accordance with the different forces operating in each region. When the scattering electron leaves the inner region, the other target electrons are confined to the inner region. Here the R -matrix boundary radius was chosen to be $10a_0$ centered at the center of mass of the S_2 molecule; the resulting sphere encloses the entire charge density of the molecule so that the amplitudes of the various occupied and virtual target orbitals are negligible at the boundary. However, the continuum orbitals have finite amplitudes at the boundary.

In the present case, the target boundary amplitudes at $10a_0$ are less than $10^{-5}a_0^{-3/2}$ for the occupied and virtual orbitals. Inside the R -matrix sphere, the electron-electron correlation and exchange interactions are strong. Short-range correlation effects are important for accurate prediction of large-angle elastic scattering, and exchange effects are important for spin-forbidden excitation cross sections.

A multicentered CI wave-function expansion is used in the inner region. The calculation in the inner region is similar to a bound-state calculation, which involves the solution of an eigenvalue problem for $(N + 1)$ electrons in the truncated space, where there are N target electrons and a single scattering electron. Outside the sphere, only long-range multipolar interactions between the scattering electron and the various target states are included. Since only direct potentials are involved in the outer region, a single-center approach is used to describe the scattering electron via a set of coupled differential equations. The R matrix is a bridge between the two regions. It describes how the scattering electron enters the inner region and how it leaves. In the outer region, the R matrix on the boundary is propagated outward [24,25] until the inner-region solutions can be matched with asymptotic solutions, thus yielding the physical observables such as cross sections.

In the polyatomic implementation of the UK molecular R -matrix code [16,17], the continuum molecular orbitals are constructed from atomic Gaussian-type orbitals (GTOs) using basis functions centered on the center of gravity of the molecule. The main advantage of GTOs is that integrals involving them over all space can be evaluated analytically in closed form. However, a tail contribution is subtracted to yield the required integrals in the truncated space defined by the inner region [16].

The target molecular orbital space is divided into core (inactive), valence (active), and virtual orbitals. The target molecular orbitals are supplemented with a set of continuum orbitals, centered on the center of gravity of the molecule. The continuum basis functions used in polyatomic R -matrix calculations are Gaussian functions and do not require fixed boundary conditions. First, target and continuum molecular orbitals are orthogonalized using Schmidt orthogonalization. Then symmetric or Löwdin orthogonalization is used to orthogonalize the continuum molecular orbitals among themselves and remove linearly dependent functions [16,26]. In general and in this work, all calculations are performed within the fixed-nuclei approximation.

In the inner region, the wave function of the scattering system, consisting of target plus scattering electron, is written using the CI expression:

$$\Psi_k^{N+1} = A \sum_i \phi_i^N(x_1, \dots, x_N) \sum_j \xi_j(x_{N+1}) a_{ijk} + \sum_m \chi_m(x_1, \dots, x_N, x_{N+1}) b_{mk}, \quad (1)$$

where A is an antisymmetrization operator, x_N is the spatial and spin coordinates of the N th electron, ϕ_i^N represents the i th state of the N -electron target, ξ_j is a continuum orbital spin-coupled with the scattering electron, and k refers to a particular R -matrix basis function. Coefficients a_{ijk} and b_{mk}

are variational parameters determined as a result of the matrix diagonalization.

The first sum runs over the 20 target states of S₂ included in the present calculation, which are represented by a CI expansion. To obtain reliable results, it is important to maintain a balance between the N -electron target representation, ϕ_i^N , and the $(N + 1)$ electron-scattering wave function. The summation in the second term of Eq. (1) runs over configurations χ_m , where all electrons are placed in target-occupied and virtual molecular orbitals. The choice of appropriate χ_m is crucial in this process [27]. These are known as L^2 configurations and are needed to account for orthogonality relaxation and for correlation effects arising from virtual excitation to higher electronic states that are excluded in the first expansion. The basis for the continuum electron is parametrically dependent on the R -matrix radius and provides a good approximation to an equivalent basis of orthonormal spherical Bessel functions [28].

We have used $39a_g$, $20b_{2u}$, $20b_{3u}$, $16b_{1g}$, $23b_{1u}$, $18b_{3g}$, $18b_{2g}$, and $6a_u$ continuum orbitals for S₂. The target and the continuum orbitals of a particular symmetry form an orthonormal set in the inner region; for example, the $5a_g$ orbitals of the target and $39a_g$ orbitals of the continuum are orthonormal to each other. The configuration state functions (CSFs) in the second term in Eq. (1) were constructed by allowing the scattering electron to occupy any of the target occupied or virtual orbitals. This term is responsible for the polarization effects in the one-state CI calculation also.

B. S₂ target and scattering model

The molecule S₂ is a linear open-shell system that has ground state $X^3\Sigma_g^-$ in the $D_{\infty h}$ point group, which is reduced to the D_{2h} point group when the symmetry is lowered. The point group D_{2h} is the highest Abelian group in our codes. The results are reported in the natural symmetry point group as well as in the D_{2h} point group for the sake of convenience. We used a double zeta plus polarization (DZP) Gaussian basis set [29] contracted as (12,8,1)/(6,4,1) for S. We avoided using diffuse functions as these would extend outside the R -matrix box, which may cause linear dependency problems. We first performed a SCF calculation for the ground state of the S₂ molecule with the chosen DZP basis set and obtained a set of occupied and a set of virtual orbitals.

The Hartree-Fock electronic configuration for the ground state is $1\sigma_g^2 \cdots 5\sigma_g^2 1\sigma_u^2 \cdots 4\sigma_u^2 1\pi_u^4 1\pi_g^4 2\pi_u^4 2\pi_g^2$, which gives rise to the lowest-lying $X^3\Sigma_g^-$, $a^1\Delta_g$, and $b^1\Sigma_g^+$ states.

The energy of the occupied $2\pi_g$ orbital is -10.02 eV and by Koopman's theorem it is the first ionization energy. Since the SCF procedure is inadequate to provide a good representation of the target states, we improve the energy of the ground as well as the excited states by using CI wave functions. A CI approach is energetically much superior to a calculation based on a SCF model. This lowers the energies and the correlation introduced provides a better description of the target wave function and excitation energies. This also gives a better description of the charge density, which is important in determining quadrupole and transition moments of the transition in the target states. In our limited CI model, we keep 20 electrons frozen in the $1\sigma_g^2 2\sigma_g^2 3\sigma_g^2 1\sigma_u^2 2\sigma_u^2 3\sigma_u^2 1\pi_u^4 1\pi_g^4$ configuration and allow the remaining 12 electrons to move freely in molecular orbitals $4\sigma_g$, $5\sigma_g$, $4\sigma_u$, $5\sigma_u$, $2\pi_u$, and $2\pi_g$. The CI ground-state energy for the S₂ molecule is -795.03737 hartree, at a bond length of $R_e = 3.676a_0$. We computed the value of vertical electronic affinity (VEA) by performing a bound-state calculation of S₂⁻ by including the continuum electron basis functions centered at the origin. The vertical electron affinity is equal to the difference in total energy of the neutral molecule and its anion at the equilibrium geometry of the neutral molecule. We detect a stable bound state of S₂⁻ with $^2\Pi_g$ symmetry having the configuration $1\sigma_g^2 \cdots 5\sigma_g^2 1\sigma_u^2 \cdots 4\sigma_u^2 1\pi_u^4 1\pi_g^4 2\pi_u^4 2\pi_g^3$ with a VEA value of 1.42 eV, which is in good agreement with the estimated experimental (adiabatic) value of about 1.67 ± 0.015 eV [30] and also with theoretical data: adiabatic electron affinity 1.48 eV and vertical electron affinity 1.32 eV [31].

To provide additional information on the charge distribution in the S₂ molecule, we have also calculated the quadrupole moment. In our CI model the absolute value of quadrupole component Q_{20} for the ground state is 0.668 a.u. The values of the ground-state energy and the ionization potential are compared with other works in Table I. The slight difference in the CI value of energy between this work and the other works is due to the change in the optimized bond length, which depends upon the basis set used.

In Table II, we list the quadrupole moment of each state (Q_{20}), N , the number of CSFs, and the vertical excitation energies for the target states. We have good agreement with the calculation of Tashiro [11], and reasonable agreement with [7,9,10] for vertical excitation energies.

We have included 20 target states (2 of 1A_g , 1 of $^3B_{2u}$, 1 of $^1B_{2u}$, 1 of $^3B_{3u}$, 1 of $^1B_{3u}$, 1 of $^3B_{1g}$, 1 of $^1B_{1g}$, 2 of $^3B_{1u}$, 2 of $^1B_{1u}$, 1 of $^3B_{3g}$, 1 of $^1B_{3g}$, 1 of $^3B_{2g}$, 1 of $^1B_{2g}$, 2 of 3A_u , and 2 of 1A_u) in the trial wave function describing the electron plus target system. However, excitation cross sections

TABLE I. Properties of the S₂ target, ground-state energy (in a.u.), the rotational constant (B_e , in cm⁻¹), SCF at bond length $R_e = 3.538a_0$, and CI at bond length $R_e = 3.676a_0$.

	Present work		Previous results ^a ($R_e = 3.57a_0$)		Previous results ^b ($R_e = 3.9657a_0$)	
	SCF	CI	SCF	CI	SCF	VCI
E	-794.99633	-795.03737	-795.00038	-795.14768	-793.2831	-793.2758
B_e	0.301	0.280	0.299	0.292	0.2636	0.2396

^aReference [6].

^bReference [7].

TABLE II. The vertical excitation energies (eV), quadrupole moments (Q_{20} in a.u.), and the number of configuration state functions (CSFs), N , for the target states of S_2 at bond length $R_e = 3.676a_0$. The experimental values, from [7], are given in square brackets.

State $C_{2v} / C_{\infty v}$	Present work (eV)	Ref. [11] (eV)	Ref. [7] (eV)	Ref. [9] (eV)	Ref. [10] (eV)	Q_{20} (a.u.)	N
$X^3B_{1g} / X^3\Sigma_g^-$	0.0					0.668	48
$a(^1A_g, ^1B_{1g}) / a^1\Delta_g$	0.603	0.60	0.674 [0.583]	0.675	0.55	0.599	60/36
$b^1A_g / b^1\Sigma_g^+$	0.912	0.92	1.214 [1.054]	1.214	0.99	0.572	60
$c^1A_u / c^1\Sigma_u^-$	2.808	2.77	2.145 [2.480]	2.145	2.45	0.894	36
$A(^3A_u, ^3B_{1u}) / A'^3\Delta_u$	2.950	2.93	2.269 [2.600]	2.269	2.59	0.882	48/48
$A^3B_{1u} / A^3\Sigma_u^+$	3.047	3.03	2.343 [2.724]	2.343	2.58	0.880	48
$B(^3B_{2g}, ^3B_{3g}) / B'^3\Pi_g$	4.840	4.84	4.389 [4.377]	4.390	4.36	4.127	48/48
$B''(^3B_{2u}, ^3B_{3u}) / B''^3\Pi_u$	4.945	5.03	4.364 [3.930]	4.364	3.81	4.670	48/48
$B^3A_u / B^3\Sigma_u^-$	5.296		4.750 [3.929]	4.750	3.89	0.9152	48
$e(^1B_{2g}, ^1B_{3g}) / e^1\Pi_g$	5.786		5.332	5.493	5.62	3.9255	40/40
$^1B_{2u}, ^1B_{3u} / ^1\Pi_u$	5.866		5.158	5.158	4.37	4.507	40/40
$f(^1A_u, ^1B_{1u}) / f^1\Delta_u$	6.8		6.162 [5.158]	6.162	5.56	0.850	44/36
$^1B_{1u} / ^1\Sigma_u^+$	7.650		7.402 [5.592]		5.55	0.700	44

are reported only for three excited states ($a^1\Delta_g$, $b^1\Sigma_g^+$, and $B^3\Sigma_u^-$). Calculations were performed for doublet and quartet scattering states with $A_g, B_{2u}, B_{3u}, B_{1g}, B_{1u}, B_{3g}, B_{2g}$, and A_u symmetries. Continuum orbitals up to $l = 4$ (g -partial wave) were included in the scattering calculation.

III. RESULTS

A. Elastic and inelastic total cross sections

The ground-state electronic configuration of S_2 has two unpaired π_g electrons. Due to vacancy in the $2\pi_g$ orbital of the ground state of S_2 , the scattering electron can occupy it, forming a stable anionic ground state of S_2 with symmetry $^2\Pi_g$. In our 20-state model, we found an R -matrix pole at -795.089545 a.u. at R_e in the scattering symmetry $^2\Pi_g$, which is lower than the energy -795.037371 a.u. of the ground state $X^3\Sigma_g^-$ of S_2 , which indicates the detection of an anionic bound state. We calculated the bound-state energies of this anionic $^2\Pi_g$ state at different bond lengths by performing an L^2 -type calculation. The potential energy curves of the $^3\Sigma_g^-$ state of the S_2 molecule and the $^2\Pi_g$ state of the S_2^- anion are shown in Fig. 1. The anion is stable at all the bond lengths. This yields a vertical electron affinity of 1.42 eV at R_e . From Fig. 1, we find that the equilibrium bond length for the ground state of the S_2^- anion is $4.0a_0$. The S-S bond length is about 8.8% elongated in the S_2^- anionic state because the extra electron is in a Π_g^* orbital.

In Fig. 2, we have summed the contribution of doublet and quartet symmetries for 20-state calculations. In this figure we notice one peak in the cross sections at 2.6 eV. The eigenphase sum shows a sudden jump of π rad centered at this position. This resonance belongs to degenerate ($^2B_{2u}$ and $^2B_{3u}$) $^2\Pi_u$ symmetry. The retention of a large number of closed electronic excitation channels in the 20-state model provides the necessary polarization potential in an *ab initio* way; this polarization potential is critical in determining the resonance parameters of the detected resonances.

In Figs. 3 and 4 we have shown the inelastic cross sections from the ground state to the three physical states, with vertical excitation thresholds along with their quadrupole moments, and the number of CSFs included in the CI expansion are given in Table II.

In Fig. 3 we notice sharp peaks at 2.6 eV in the cross section of $X^3\Sigma_g^- - a^1\Delta_g$ and $X^3\Sigma_g^- - b^1\Sigma_g^+$ transitions. Each of these resonances has a width of 0.11 eV. These resonances belong to degenerate ($^2B_{2u}$ and $^2B_{3u}$) $^2\Pi_u$ symmetries. We assign a common configuration $(4\sigma_g)^2(4\sigma_u)^2(5\sigma_g)^2(2\pi_u)^4(2\pi_g)^3$ to these resonances, which is obtained from an attachment of the scattering electron to the excited $c^1\Sigma_u^-$, $A'^3\Delta_u$, and $A^3\Sigma_u^+$ states of S_2 with outer configuration $(4\sigma_g)^2(4\sigma_u)^2(5\sigma_g)^2(2\pi_u)^4(2\pi_g)^2$. The resonance properties of these peaks are also given in Table III. In Fig. 3, we have compared our results with another R -matrix calculation [11], which is in good agreement. We have also shown the electronic excitation results, for e -O $_2$ scattering [32] and e -SO scattering [33], using the R -matrix method. In contrast to O $_2$ results for both excitation processes, there is marked resonance structure

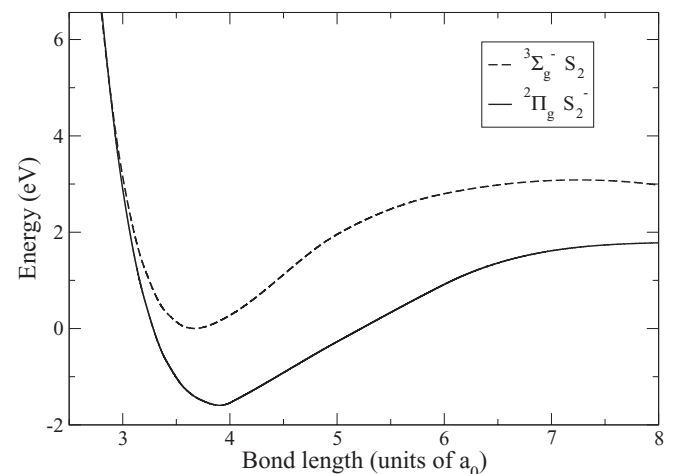


FIG. 1. Ground-state potential energy curves of S_2 and S_2^- molecules: dashed curve, S_2 ; solid curve, S_2^- .

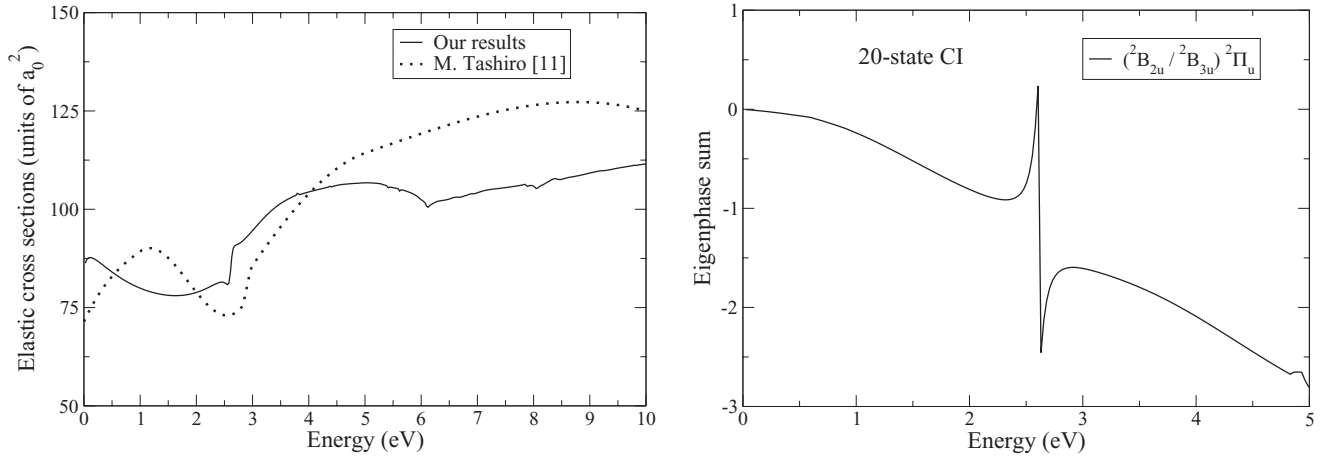


FIG. 2. Elastic cross sections of the electron impact on the S₂ molecule. (left) Dotted curve, results of Tashiro [11] at bond length $R_e = 3.7a_0$; solid curve, our results for 20-state CI calculations at bond length $R_e = 3.676a_0$. (right) Eigenphase sum of $(^2B_{2u}/^2B_{3u})^2\Pi_u$ symmetry for 20-state CI calculation.

in the case of S₂ around 2.6 eV, and also in the SO molecule at 4 eV. In general, the cross sections for S₂ are slightly larger because S₂ is a bigger molecule than O₂ or SO.

Figure 4 depicts the excitation cross section for the optically allowed transition $X^3B_{1g}(X^3\Sigma_g^-) \rightarrow B^3A_u(B^3\Sigma_u^-)$ and also shows the comparison with [11] and [8]. We have also shown the contribution from each symmetry (doublets and quartets) in excitation cross sections for this X - B transition. We have predicted a total of six resonances (two resonances in 2A_u , two in $^2B_{1g}$, one in 4A_u , and one in $^4B_{1g}$). For this transition, the transition moment is compared with the results of [8] in Table IV. The resonance positions and widths are shown in Table V. The Born correction is applied for this dipole transition in our results. This takes care of the partial-wave contribution ($l > 4$) to the scattering cross section in the R -matrix results.

B. Dissociative electron attachment

The study of dissociative electron attachment (DEA) correlates various resonances to the possible reaction channels. In

DEA experiments, the fragment negative ion yield is measured as a function of the kinetic energy of the incident electron. Due to the mechanism of resonant electron capture by the neutral molecule, a temporary negative ion is formed that may follow a dissociative decay channel, in which the negative ion so formed is sufficiently long-lived that it can be directed to a mass filter. The molecule initially in the ground state makes a vertical transition to a repulsive electronic state of the scattering system through which it dissociates. The study of DEA provides an important input in the modeling of plasmas. It is also known that the secondary electrons cause damage to DNA via DEA. The present study identifies the presence of the bound state of S₂⁻ in symmetry $^2\Pi_g$ ($^2B_{2g}$ and $^2B_{3g}$) and shape resonance in $^2\Pi_u$ ($^2B_{2u}$ and $^2B_{3u}$) symmetry. To explore the possible dissociative nature of this resonance state, we have investigated their dependence by stretching the S-S bond length from its equilibrium value to $5a_0$. This stretching mode asymptotically correlates to the following two-body fragmentation channel:

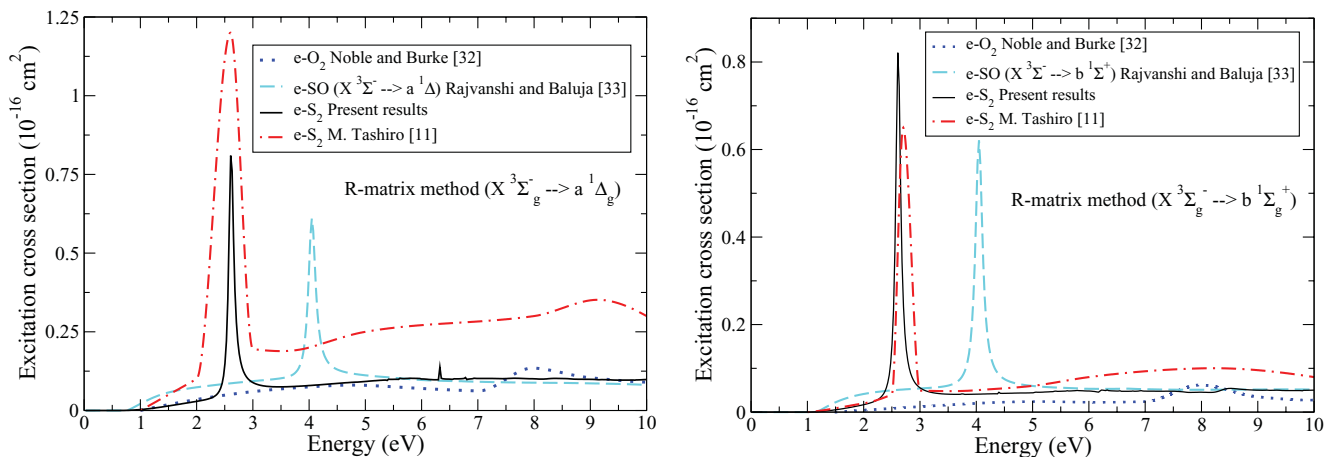


FIG. 3. (Color online) Electron-impact excitation cross sections from the ground state: $X^3\Sigma_g^-$ ($^3B_{1g}$) of the S₂ molecule to the $a^1\Delta_g$, $a^1A_g/1^1B_{1g}$ and $b^1\Sigma_g^+$ (1^1A_g), present study, solid line; Tashiro [11], dash-dotted curve; $X^3\Sigma_g^-$ of the O₂ molecule to the $a^1\Delta_g$ and $b^1\Sigma_g^+$, Noble and Burke [32], dotted curve; $X^3\Sigma^-$ of the SO molecule to the $a^1\Delta$ and $b^1\Sigma^+$, Rajvanshi and Baluja [33], dashed curve.

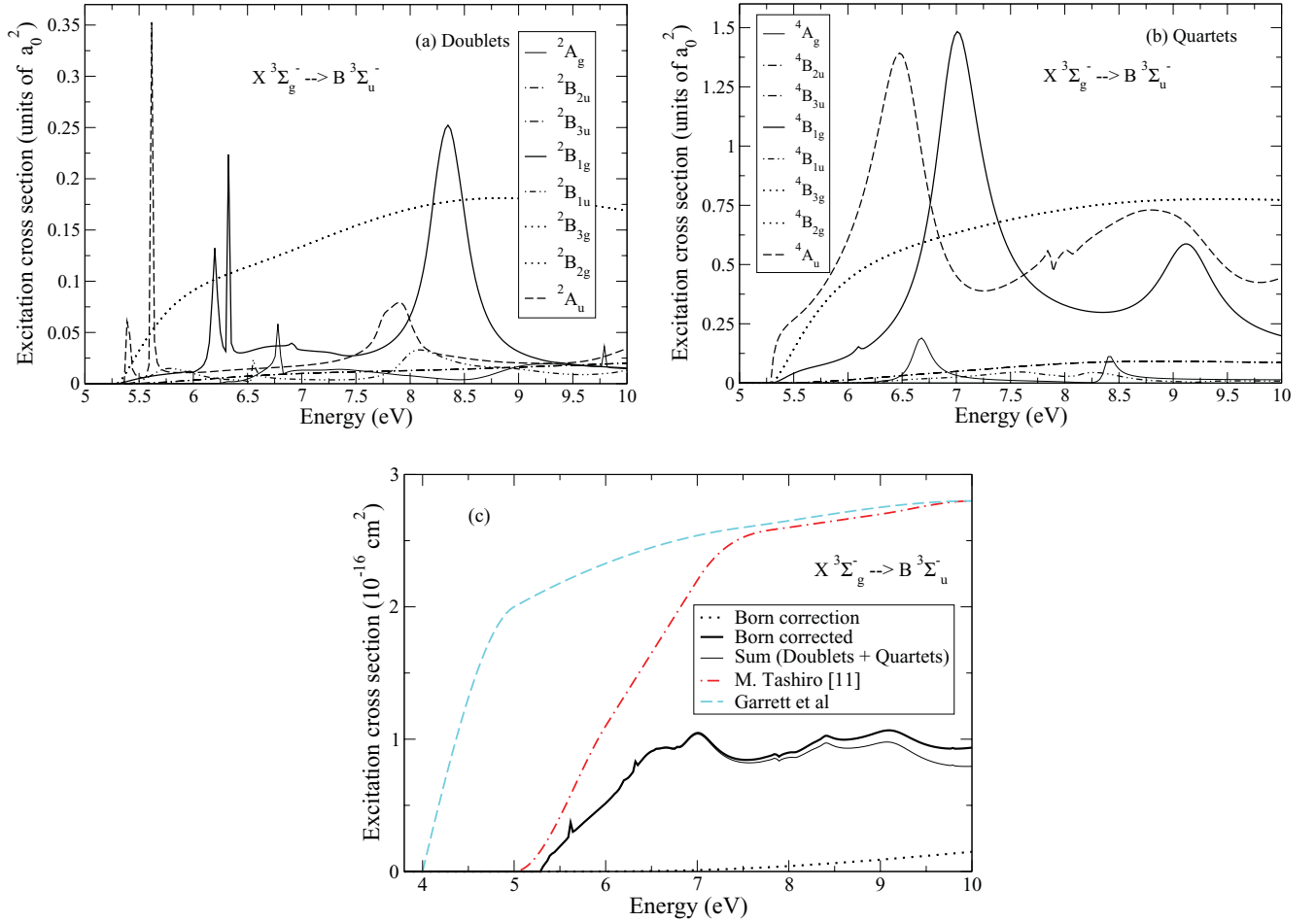


FIG. 4. (Color online) Electron-impact excitation cross sections from the ground $X^3\Sigma_g^-$ ($^3B_{1g}$) state of the S_2 molecule to the $B^3\Sigma_u^-$ (3A_u) state for 20-state calculation: contribution in the excitation cross sections from each symmetry (a) in doublets and (b) in quartets. (c) dash-dotted curve, Tashiro [11]; dashed curve, Garrett *et al.* [8]; thin solid line, total sum (doublets + quartets); dotted curve, Born correction; thick solid line, Born corrected (sum of doublets, quartets, and Born correction).

In Fig. 5, we have shown the resonance position and the resonance width as a function of stretching bond S-S in D_{2h} symmetry for $^2\Pi_u$ ($^2B_{2u}$ and $^2B_{3u}$). From Fig. 5 we observed that the resonance width and position decrease with increase in bond length of the S-S bond and they approach zero at $4.8a_0$; beyond this the resonance width and position vanish, which implies that these resonances become bound and support dissociative electron attachment. The variation of position and width of the $^2\Pi_u$ resonance with respect to the energy of the ground state as a function of internuclear distance is shown in Table VI. These data are useful to find DEA cross sections.

C. Ionization cross section

Figure 6 shows electron-impact ionization cross section of S_2 from threshold 10.02 eV to 5000 eV by using the standard formalism of the BEB model [19,20]. This formalism requires the binding energy and kinetic energy of each occupied orbital in a molecular structure calculation. The ionization cross section rises from threshold to a peak value of 7.7 \AA^2 at 63.96 eV and then shows $\ln(E/E)$ behavior as E approaches higher values. We have also shown the results of previous theoretical works [12,14] and experimental data by Freund *et al.* [13]. The molecular orbital data used in the calculation of BEB cross sections is given in Table VII, which is generated at the SCF level, and compared with theoretical results reported

TABLE III. Resonance properties of S_2 at bond length $R = 3.676a_0$.

Electronic configuration of resonant state	E_r (eV)	Γ_r (eV)	Type of resonance	Parent state
$1(\sigma_g)^2 \dots 5(\sigma_g)^2 1(\sigma_u)^2 \dots 4(\sigma_u)^2 1(\pi_u)^4 1(\pi_g)^4 2(\pi_u)^4 2(\pi_g)^3 \cdot 2\Pi_u$	2.63	0.11	Shape resonance	$a^1\Delta_g$
$1(\sigma_g)^2 \dots 5(\sigma_g)^2 1(\sigma_u)^2 \dots 4(\sigma_u)^2 1(\pi_u)^4 1(\pi_g)^4 2(\pi_u)^4 2(\pi_g)^3 \cdot 2\Pi_u$	2.63	0.11	Shape resonance	$b^1\Sigma_g^+$

TABLE IV. Comparison of transition moments of allowed transitions for S₂, at bond length $R_e = 3.676a_0$, with [8].

Transition	Transition moment ¹ (a.u.)	Transition moment (this work) (a.u.)
${}^3\Sigma_g^- \rightarrow {}^3\Pi_u$	0.033	0.046
${}^3\Sigma_g^- \rightarrow {}^3\Sigma_u^-$	1.1	0.886

¹Garrett *et al.* [8].

by Kim *et al.* [14] using the binary-encounter-Bethe model with a Gaussian basis set (6-311-G set) provided by the GAMESS code. For an open-shell S₂ molecule, they [14] found that the unrestricted Hartree-Fock method produced more realistic orbital energies for valence orbitals than the restricted open-shell Hartree-Fock method, which they took as the electron binding energies as prescribed by the Koopman theorem. The BEB ionization cross section σ is obtained by summing over each orbital cross section σ_i , where

$$\sigma_i(t) = \frac{s}{t+u+1} \left[\frac{1}{2} \left(1 - \frac{1}{t^2} \right) \ln t + \left(1 - \frac{1}{t} \right) - \frac{\ln t}{t+1} \right], \quad (3)$$

where $t = T/B$, $u = U/B$, and $s = 4\pi a_0^2 N(R/B)^2$. Here R is the Rydberg energy, T is the kinetic energy of the incident electron, U is the orbital kinetic energy, N is the electron occupation number, and B is the binding energy of the orbital.

D. Differential cross section

The evaluation of the differential cross section (DCS) provides a more stringent test for any theoretical model. The rotational excitation cross sections for electron impact on a neutral molecule can be calculated from the scattering parameters of elastic scattering in the fixed-nuclei approximation, provided the nuclei are assumed to be of infinite mass [34]. In particular, starting from an initial rotor state $J = 0$, the sum of all transitions from the $J = 0$ level to a high enough J value for convergence is equivalent to the elastic cross section in the fixed-nuclei approach. We have employed this methodology to extract rotationally elastic and rotationally inelastic cross sections from the K -matrix elements calculated in the one-state

TABLE V. Resonance properties of S₂ molecule for $X^3\Sigma_g^- \rightarrow B^3\Sigma_u^-$ transition at bond length $R = 3.676a_0$.

Symmetry	Position E_r (eV)	Width Γ_r (eV)
2A_u	5.39	0.048
2A_u	5.62	0.036
${}^2B_{1g}$	6.20	0.06
${}^2B_{1g}$	6.33	0.03
4A_u	6.47	0.52
${}^4B_{1g}$	7.00	0.45

R -matrix model. The DCS for a general polyatomic molecule is given by the familiar expression

$$\frac{d\sigma}{d\Omega} = \sum_L A_L P_L(\cos\theta), \quad (4)$$

where P_L is a Legendre polynomial of order L . The A_L coefficients have already been discussed in detail [35]. For a polar molecule this expansion over L converges slowly. To circumvent this problem, we use the closure formula

$$\frac{d\sigma}{d\Omega} = \frac{d\sigma^B}{d\Omega} + \sum_L (A_L - A_L^B) P_L(\cos\theta). \quad (5)$$

The superscript B denotes that the relevant quantity is calculated in the Born approximation with an electron-point dipole interaction. The convergence of the series is now rapid since the contribution from the higher partial waves to the DCS is dominated by the electron-dipole interaction. The quantity $\frac{d\sigma}{d\Omega}$ for any initial rotor state $|Jm\rangle$ is given by the sum over all final rotor states $|J'm'\rangle$,

$$\frac{d\sigma}{d\Omega} = \sum_{J'm'} \frac{d\sigma}{d\Omega}(Jm \rightarrow J'm'), \quad (6)$$

where J is the rotational angular momentum and m is its projection on the internuclear axis. To obtain converged results, the maximum value is $J' = 5$. We have calculated the DCS by using the POLYDCS program of Sanna and Gianturco [36] that requires basic molecular input parameters along with K matrices evaluated in a particular scattering calculation. We have used this code to compute the DCS in a one-state CI

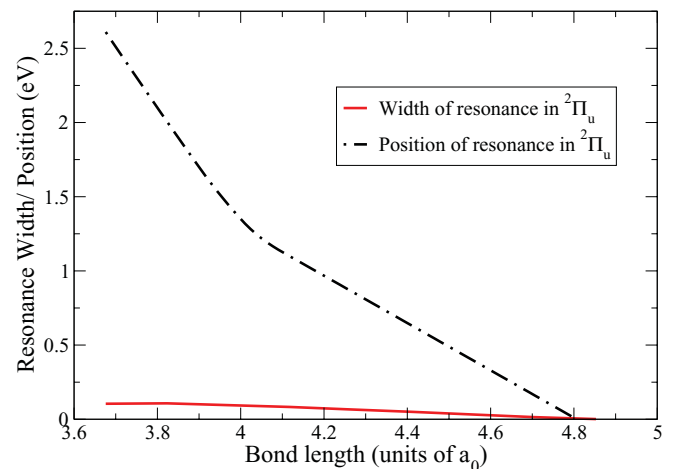


FIG. 5. (Color online) Variation of resonance width and position with bond length: dashed curve, position of resonance (${}^2\Pi_u$); solid curve, width of resonance (${}^2\Pi_u$).

TABLE VI. Position and width of the $^2\Pi_u$ resonance with respect to the energy of the ground state as a function of internuclear distance, R (a_0).

R (a_0)	Position (E_r) (eV)	Width Γ_r (eV)
3.676	2.63	0.11
3.7	2.51	0.108
3.8	2.10	0.106
3.9	1.70	0.102
4.0	1.35	0.091
4.1	1.13	0.082
4.2	0.96	0.066
4.4	0.65	0.052

model. Since S_2 is an open-shell molecule having $X^3\Sigma_g^-$ as its ground state, the spin coupling between this target state and the spin of the incoming electron allows two spin-specific channels, namely the doublet (D) and quartet (Q) couplings. The spin-averaged DCSs for elastic electron scattering from the S_2 molecule are calculated by using the statistical weights $2/6$ for doublet and $4/6$ for quartet scattering channels. We then use Eq. (3) as follows to calculate the DCS:

$$\frac{d\sigma}{d\Omega} = \frac{1}{3} \left[2 \left(\frac{d\sigma}{d\Omega} \right)^Q + \left(\frac{d\sigma}{d\Omega} \right)^D \right], \quad (7)$$

where $\left(\frac{d\sigma}{d\Omega} \right)^{Q,D}$ represents DCSs for quartet and doublet cases, respectively.

In Fig. 7 we have shown the spin-averaged DCS calculated in the one-state R -matrix model at different energies. We have compared our results with the results of Tashiro [11], who used the angular momentum representation of the T -matrix elements for the first Born approximation. Our results are in reasonable agreement with the results of Tashiro [11] at 7, 10, and 13 eV. In this figure we have also shown the state-to-state rotational components of DCSs to investigate the effect of convergence of a DCS with respect to the increasing value

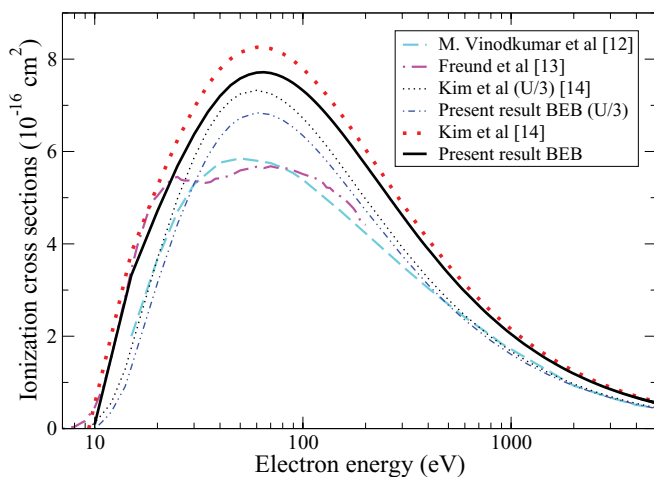


FIG. 6. (Color online) Electron-impact BEB ionization cross sections of the S_2 molecule: dashed curve, Vinodkumar *et al.* [12]; dotted curve, Kim *et al.* (theoretical) [14]; dash-dotted curve, Freund *et al.* (experiment) [13]; thick solid line, our BEB model.

 TABLE VII. S_2 molecular orbital binding and average kinetic energies for DZP basis set at equilibrium geometry: $|B|$ is binding energy, U is kinetic energy, and N is occupation number.

Molecular orbital	Our results		Previous results		N
	$ B $ (eV)	U (eV)	$ B ^a$ (eV)	U^a (eV)	
$1\sigma_g(1a_g)$	2503.90	3296.83			2
$1\sigma_u(1b_{1u})$	2503.89	3296.83			2
$2\sigma_g(2a_g)$	245.38	509.0	245.93	509.43	2
$2\sigma_u(2b_{1u})$	245.37	509.25	245.92	509.43	2
$3\sigma_g(3a_g)$	182.24	477.69	182.81	478.98	2
$3\sigma_u(3b_{1u})$	182.21	478.32	182.80	478.55	2
$1\pi_u(1b_{2u})$	182.15	478.48	182.72	478.98	2
$1\pi_u(1b_{3u})$	182.15	478.48	182.72	478.98	2
$1\pi_g(1b_{3g})$	182.15	478.51	182.72	478.28	2
$1\pi_g(1b_{2g})$	182.15	478.51	182.72	478.28	2
$4\sigma_g(4a_g)$	29.89	62.92	29.25	60.84	2
$4\sigma_u(4b_{1u})$	21.67	70.87	22.35	72.54	2
$5\sigma_g(5a_g)$	14.08	57.54	13.42	54.39	2
$2\pi_u(2b_{2u})$	12.93	43.91	12.59	43.13	2
$2\pi_u(2b_{3u})$	12.93	43.91	12.59	43.13	2
$2\pi_g(2b_{3g})$	5.01	54.52	4.68	56.46	1
$2\pi_g(2b_{2g})$	5.01	54.52	4.68	56.46	1

^aKim *et al.* [14]

of the final rotational angular momentum J' . Because of the nonpolar nature of the S_2 molecule, the contribution of $0 \rightarrow 1,3,5$ is much smaller (less than $0.1 \times 10^{-16} \text{ cm}^2/\text{sr}$) than the contribution from the even J' values. The component $0 \rightarrow 0$ is most dominant among all the components because it represents rotational elastic scattering. The contribution of the $0 \rightarrow 2$ component comes mainly from the quadrupole moment of the molecule.

In addition, the data on DCS are further used to calculate the momentum-transfer cross section (MTCS) that shows the importance of backward angle scattering. Since the DCSs are not very sensitive to correlation effects for backward scattering, we expect our MTCS to be quite reliable in the 0.01–10 eV range. These are calculated in the one-state CI model with spin averaging. MTCS provides a useful input in solving the Boltzmann equation for the electron distribution function. In contrast to the diverging nature of DCSs in the forward direction, MTCSs show no singularity due to the weighting factor $(1 - \cos \theta)$, where θ is the scattering angle. This factor vanishes as $\theta \rightarrow 0$. The MTCS is useful in the study of electrons drifting through a molecular gas. When a swarm of electrons travels through a molecular gas under the influence of an electric field, several transport observables, such as the diffusion coefficient D and the mobility μ , can be obtained if we have a knowledge of the momentum-transfer cross sections. In Fig. 8, we have shown the calculated MTCSs at different energies for electron collision with a S_2 molecule.

E. Effective collision frequency of electrons

The effective electron-neutral collision frequency $\langle \nu \rangle$, which is averaged over a Maxwellian distribution, can be obtained from the momentum-transfer cross section $Q^{(m)}(\nu)$

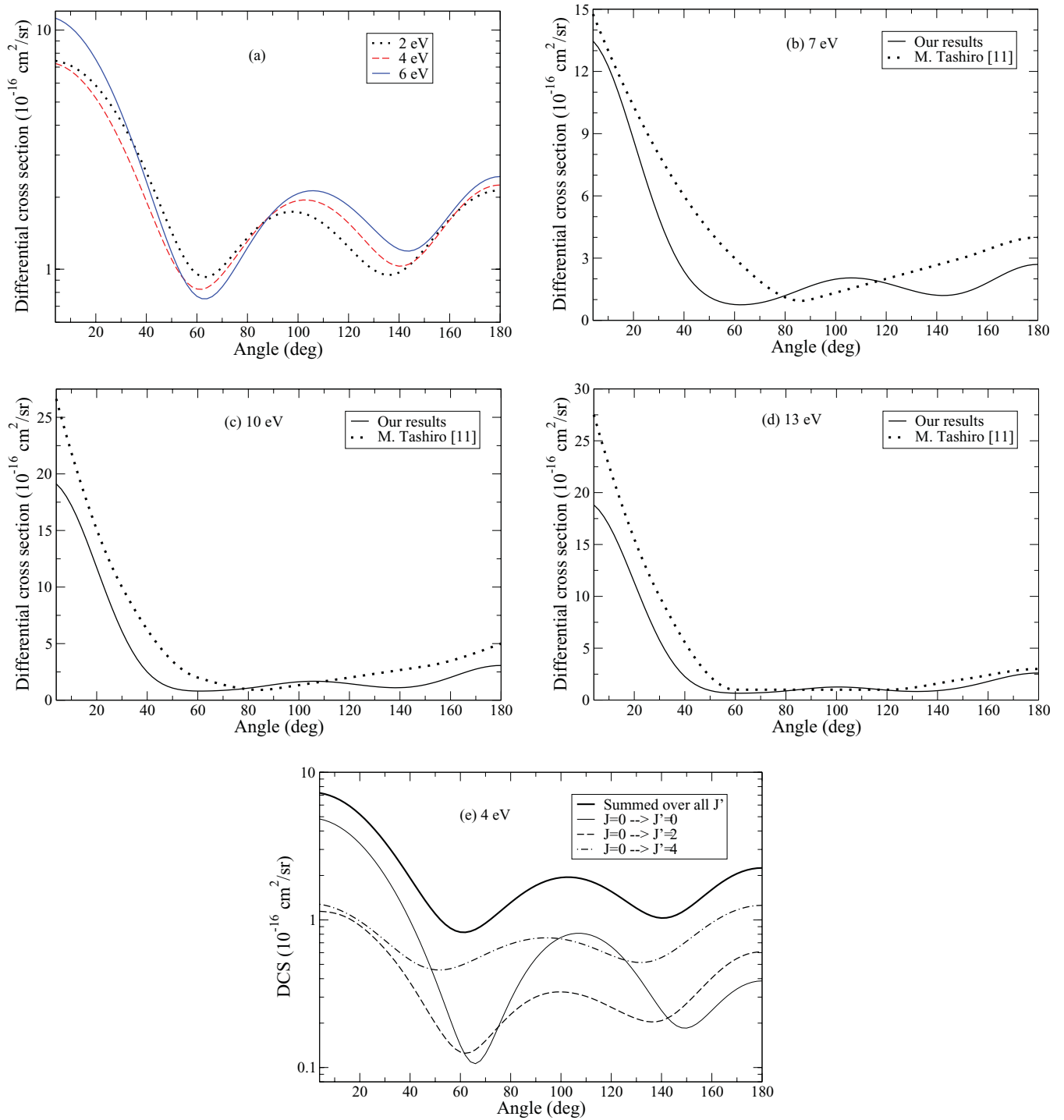


FIG. 7. (Color online) (a) Differential cross sections (DCSs) at 2, 4, and 6 eV. Comparison of DCS, at (b) 7, (c) 10, and (d) 13 eV, with results of Tashiro [11]; dotted curve, Tashiro [11]; solid curve, present result (with spin average) for one-state CI model at R_e ; (e) DCS at 4 eV for state-to-state rotational components of DCS for initial state $J = 0$ to final state $J' = 0, 2, 4$.

as follows [37]:

$$\langle v \rangle = \frac{8}{3\pi^{1/2}} N \left(\frac{m_e}{2kT_e} \right)^{5/2} \int_0^\infty v^5 Q^{(m)}(v) \exp\left(\frac{-m_e v^2}{2kT_e}\right) dv, \quad (8)$$

where m_e and T_e are the electron mass and temperature, respectively; k is Boltzmann's constant; v is the velocity; and N is the number density of the gas particles. The averaging is

over a Maxwellian speed distribution function for an electron temperature T_e , which is given by

$$f(v) = 4\pi v^2 \left(\frac{m_e}{2\pi kT_e} \right)^{3/2} \exp\left(\frac{-m_e v^2}{2kT_e}\right). \quad (9)$$

This type of collision frequency is often used to evaluate the energy transfer between particles. Alternatively, the effective

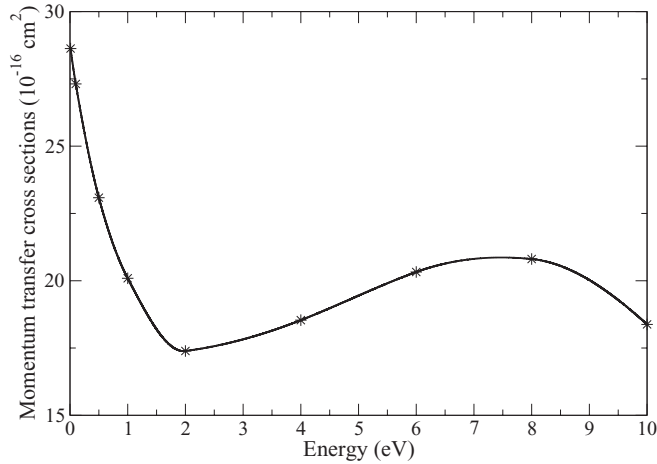


FIG. 8. Momentum transfer cross sections, at different energies, with spin average of S_2 molecule ground state at one-state CI level.

collision frequency for electrons can be defined from the dc conductivity as follows [37,38]:

$$\bar{v}^{-1} = \frac{8}{3\pi^{1/2}N} \left(\frac{m_e}{2kT_e} \right)^{5/2} \int_0^\infty \frac{v^3}{Q^{(m)}(v)} \exp\left(\frac{-m_e v^2}{2kT_e}\right) dv. \quad (10)$$

This explicit form of effective collision frequency \bar{v} is related to the drift velocity of electrons in a gas, insofar as a Maxwell distribution can be assumed. When $Q^{(m)}(v)$ is proportional to v^{-1} , the two effective collision frequencies, $\langle v \rangle$ and \bar{v} , agree. In Fig. 9, we have shown both types of effective collision frequencies as a function of electron temperature. It is to be noted that $\langle v \rangle$ lies higher than \bar{v} in the entire electron temperature range.

F. Scattering length

We have also evaluated scattering length in our study of electron impact on the S_2 molecule. In this procedure we have included only an s -wave approximation for the scattering electron. The scattering length is given by

$$a = \frac{-\tan \delta_0}{k}, k \rightarrow 0, \quad (11)$$

where δ_0 is the eigenphase sum corresponding to the energy ($E = 0$). In practice, we have chosen $E = 0.025$ eV to compute a . Here k is the wave number of the scattering electron.

We have calculated scattering length separately for doublets (a_D) and quartets (a_Q); the spin-averaged scattering length is given by

$$a = \left[\frac{1}{3}(a_D^2 + 2a_Q^2) \right]^{1/2}. \quad (12)$$

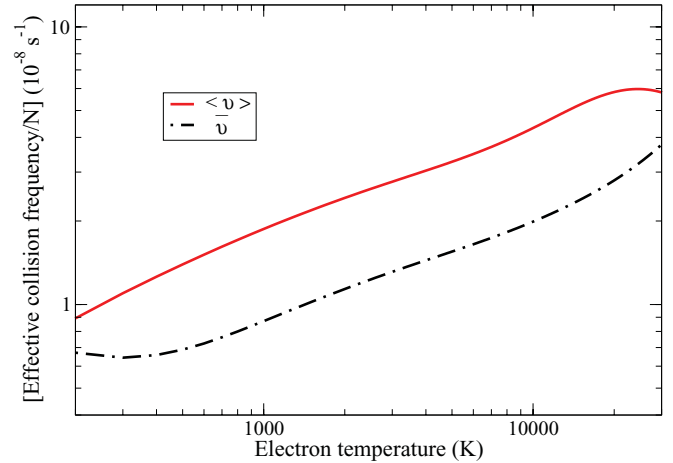


FIG. 9. (Color online) Effective collision frequency as a function of electron temperature: dashed curve, \bar{v} ; solid curve, $\langle v \rangle$.

We obtained a value of $2.615a_0$ for the scattering length. Then we evaluated the cross section $\sigma = 4\pi a^2$ corresponding to this scattering length, which is equal to $85.866a_0^2$; this result is comparable with the cross section $85.7a_0^2$ at the same energy ($E = 0.025$ eV) coming from the direct calculation (R -matrix method).

IV. CONCLUSIONS

This is a comprehensive *ab initio* study of electron impact on the S_2 molecule using the UK molecular R -matrix codes. Elastic (integrated and differential), momentum-transfer, excitation, and ionization cross sections have been presented. The results of the static-exchange, one-state CI, and 20-state close-coupling approximations are presented. We detect a stable bound state of S_2^- with a vertical electronic affinity value of 1.42 eV, which is in good agreement with the estimated experimental value of about 1.67 ± 0.015 eV. The target states are represented by including correlations via a configuration-interaction technique. Our target calculations give reasonable agreement with the calculated vertical excitation spectrum of Tashiro [11], Swope *et al.* [7], Wang *et al.* [9], and Kiljunen *et al.* [10]. We have also reported the quadrupole moment for each state. We detected two resonances, both of ${}^2\Pi_u$ symmetry, in the excitation cross sections of the states ${}^1\Delta_g$ and ${}^1\Sigma_g^+$. The dissociative nature of these resonances is explored by performing scattering calculations in which the S-S bond is stretched. These resonances support dissociative attachment, yielding S and S^- . The derived MTCS from the DCS and two types of effective collision frequencies have also been presented. We have also evaluated the scattering length of the S_2 molecule, which is equal to $2.615a_0$.

[1] K. S. Noll, M. A. McGrath, L. M. Trafton, S. K. Atreya, J. J. Caldwell, H. A. Weaver, R. V. Yelle, C. Barnett, and S. Edington, *Science* **267**, 1307 (1995).

[2] S. J. Kim, M. F. Ahearn, and S. M. Larson, *Icarus* **87**, 440 (1990).

[3] G. F. Mitchell, *Astrophys. J.* **287**, 665 (1984).

- [4] B. P. Turner, M. G. Ury, Y. Leng, and W. G. Love, *J. Illum. Eng. Soc. Winter* **26**, 10 (1997).
- [5] G. Lakshminarayana and C. G. Mahajan, *J. Quant. Spectrosc. Radiat. Transfer* **16**, 549 (1976).
- [6] A. D. Tait, M. Dixon, and K. E. Banyard, *J. Phys. B* **7**, 1908 (1974).
- [7] W. C. Swope, Y.-P. Lee, and H. F. Schaefer, *J. Chem. Phys.* **70**, 947 (1979).
- [8] B. C. Garrett, L. T. Redmon, C. W. McCurdy, and M. J. Redmon, *Phys. Rev. A* **32**, 3366 (1985).
- [9] X.-C. Wang and K. F. Freed, *J. Chem. Phys.* **86**, 2899 (1987).
- [10] T. Kiljunen, J. Eloranta, H. Kunttu, L. Khriachtchev, M. Pettersson, and M. Räsänen, *J. Chem. Phys.* **112**, 7475 (2000).
- [11] M. Tashiro, *Chem. Phys. Lett.* **453**, 145 (2008).
- [12] M. Vinodkumar, C. Limbachiya, and H. Bhutadia, *J. Phys. B* **43**, 015203 (2010).
- [13] R. S. Freund, R. C. Wetzel, and R. J. Shul, *Phys. Rev. A* **41**, 5861 (1990).
- [14] Y.-K. Kim, W. Hwang, N. M. Weinberger, M. A. Ali, and M. E. Rudd, *J. Chem. Phys.* **106**, 1026 (1997).
- [15] Y. Le Coat, L. Bouby, J. P. Guillotin, and J. P. Ziesel, *J. Phys. B* **29**, 545 (1996).
- [16] L. A. Morgan, C. J. Gillan, J. Tennyson, and X. Chen, *J. Phys. B* **30**, 4087 (1997).
- [17] L. A. Morgan, J. Tennyson, and C. J. Gillan, *Comput. Phys. Commun.* **114**, 120 (1998).
- [18] J. Tennyson, *J. Phys. B* **29**, 1817 (1996).
- [19] Y. K. Kim and M. E. Rudd, *Phys. Rev. A* **50**, 3954 (1994).
- [20] W. Hwang, Y. K. Kim, and M. E. Rudd, *J. Chem. Phys.* **104**, 2956 (1996).
- [21] C. W. McCurdy and T. N. Rescigno, *Phys. Rev. A* **39**, 4487 (1989).
- [22] *Atomic and Molecular Processes: An R-matrix Approach*, edited by P. G. Burke and K. A. Berrington (Institute of Physics Publishing, Bristol, UK, 1993).
- [23] C. J. Gillan, J. Tennyson, and P. G. Burke, *Computational Methods for Electron-Molecule Collisions*, edited by W. M. Huo and F. A. Gianturco (Plenum, New York, 1995).
- [24] K. L. Baluja, P. G. Burke, and L. A. Morgan, *Comput. Phys. Commun.* **27**, 299 (1982).
- [25] L. A. Morgan, *Comput. Phys. Commun.* **31**, 419 (1984).
- [26] B. M. Nestmann, K. Pfingst, and S. D. Peyerimhoff, *J. Phys. B* **27**, 2297 (1994).
- [27] J. Tennyson, *J. Phys. B* **29**, 6185 (1996).
- [28] A. Faure, J. D. Gorfinkiel, L. A. Morgan, and J. Tennyson, *Comput. Phys. Commun.* **144**, 224 (2002).
- [29] T. H. Dunning and P. J. Hay, *Methods of Electronic Structure Theory*, edited by H. F. Schaefer (Plenum, New York, 1977), Vol. 2.
- [30] S. Moran and G. B. Ellison, *J. Phys. Chem.* **92**, 1794 (1988).
- [31] C. Heinemann, W. Koch, G.-G. Lindner, and D. Reinen, *Phys. Rev. A* **52**, 1024 (1995).
- [32] C. J. Noble and P. G. Burke, *Phys. Rev. Lett.* **68**, 2011 (1992).
- [33] J. S. Rajvanshi and K. L. Baluja, *Phys. Rev. A* **82**, 032706 (2010).
- [34] E. S. Chang and A. Temkin, *Phys. Rev. Lett.* **23**, 399 (1969).
- [35] F. A. Gianturco and A. Jain, *Phys. Rep.* **143**, 347 (1986).
- [36] N. Sanna and F. A. Gianturco, *Comput. Phys. Commun.* **114**, 142 (1998).
- [37] Y. Itikawa, *Phys. Fluids* **16**, 831 (1973).
- [38] I. P. Shkarofsky, *Can. J. Phys.* **39**, 1619 (1961).